Journal of Anatomy

J. Anat. (2013) **222**, pp161–169 doi: 10.1111/joa.12001

Cutaneous innervation of the human face as assessed by skin biopsy

Maria Nolano,[1] Vincenzo Provitera,[1] Giuseppe Caporaso,[1] Annamaria Stancanelli,[1] Massimo Leandri,[2] Antonella Biasiotta,[3] Giorgio Cruccu,[3] Lucio Santoro[4] and Andrea Truini[3]

[1]*'Salvatore Maugeri' Foundation IRCCS, Medical Center of Telese Terme (BN), Telese Terme, Italy*
[2]*Interuniversity Centre for Pain Neurophysiology, University of Genoa, Genoa, Italy*
[3]*Department of Neurological Sciences, 'La Sapienza' University, Rome, Italy*
[4]*Department of Neurological Sciences, University of Naples 'Federico II', Naples, Italy*

Abstract

The morphology of cutaneous sensory and autonomic innervation in human trigeminal territory is still unknown. The aim of this study is to describe facial cutaneous innervation using skin biopsy. This new tool could be useful in understanding the mechanisms underlying several facial pain conditions. In 30 healthy subjects, we quantified epidermal nerve fibers (ENFs) and dermal myelinated fibers (MFs) in V1, V2 and V3, using indirect immunofluorescence and confocal microscopy applied to 2-mm punch skin biopsies from areas adjacent to the eyebrow, upper and lower lip. Using selective markers, we also evaluated the distribution of peptidergic, cholinergic and noradrenergic fibers. Facial skin appeared abundantly innervated and rich in annexes. The ENF density decreased and the MF density increased, moving from the supraorbital to the perioral skin. Noradrenergic sudomotor fibers were particularly and constantly expressed compared with other body sites. Distribution of vasoactive intestinal peptide-immunoreactive (VIP-ir) fibers appeared peculiar for their constant presence in the subepidermal neural plexus – in close contact, but without colocalization with calcitonin gene related peptide (CGRP) and substance P (Sub-P)-ir fibers. Finally, in perioral skin samples, we observed striated muscle fibers with their motor nerves and motor endplates. Our work provides the first morphological study of human facial cutaneous innervation, highlighting some unique features of this territory. Quantification of unmyelinated and myelinated fibers on 2-mm punch biopsies appeared to be feasible and reliable. Facial skin biopsy may be a new approach with which to study and to better characterize facial pain syndromes.

Key words: epidermal nerve fibers; myelinated fibers; skin biopsy; trigeminal innervation.

Introduction

Skin biopsy is a minimally invasive tool used to assess sensory (Kennedy & Wendelschafer-Crabb, 1993) and autonomic (Kennedy et al. 1994; Donadio et al. 2006) nerve fibers. Using this method, it is possible to describe in detail the different sensory receptors and nerve subtypes that populate the hairy and glabrous skin. This research has moved the field a step forward in the understanding of the physiology of the nervous system at its extreme periphery. The main clinical application of skin biopsy is the diagnosis of small-fiber neuropathy – a diagnosis which is made using the well standardized technique of counting the epidermal nerve fibers (ENFs) in a 3-mm punch biopsy from the distal leg (Lauria et al. 2010a,b). ENFs are C and A delta fiber endings which are involved in thermal, mechano-, and pain perception, originating in the subepidermal neural plexus (SNP) and reaching the epidermis as free nerve endings. In addition, A beta fibers, mostly involved in mechanoreception, end in the skin as myelinated fibers (MF) destined for dermal corpuscles in glabrous skin and for hair follicles in hairy skin. MF quantification, which appears reliable in dermal papillae of glabrous skin (Nolano et al. 2003), where these fibers show a regular and predictable pattern, is still a challenging task in hairy skin (Provitera et al. 2007; Doppler et al. 2012).

Skin biopsy can be applied to virtually any body area; however, it has never been applied to the trigeminal region. In fact, the evaluation of the trigeminal pathway relies on neurophysiological methods such as blink reflex to investigate A beta fibers, and laser evoked potentials (LEPs)

Correspondence
Maria Nolano, Department of Neurology, 'S. Maugeri' Foundation I.R.C.C.S., Via Bagni Vecchi, 1 – 82037 Telese Terme, BN, Italy.
T: + 39 0824 909111; F: + 39 0824 909614; E: maria.nolano@fsm.it

Accepted for publication *25 September 2012*
Article published online *18 October 2012*

to investigate A delta and C afferents (Truini & Cruccu, 2008; Cruccu et al. 2010). Importantly, the known difficulties in C-LEP recording limit the applicability of this technique (Truini et al. 2008; Cruccu et al. 2010).

We planned this study to evaluate human facial cutaneous innervation in the three trigeminal divisions using 2-mm punch skin biopsies, based on the assumption that skin biopsy of the face could yield additional information on the different sets of sensory and autonomic fibers which is currently unattainable from routine neurophysiological investigations. Moreover, this approach may improve our insight into the mechanisms underlying several facial neuralgic conditions such as trigeminal neuralgia and trigeminal neuropathy. For this purpose, we quantified ENF with standardized procedures (Lauria et al. 2010a). MFs were also quantified, applying a new and easy method which we compared with an unbiased stereological assay (Howell et al. 2002).

Materials and methods

Subjects

We studied a cohort of 30 healthy volunteers (recruited from among the Authors, Authors' colleagues and relatives) made up of 15 males and 15 females (mean age 58.2 ± 13.7; range 24–78) without symptoms or signs of neurological disease. None of the subjects had a history of excessive consumption of alcohol. Metabolic and endocrine disorders were ruled out by means of blood test screening (cell blood count, fasting glucose levels, glucose tolerance test, blood urea nitrogen, alanine and aspartate aminotransferase, and thyroid hormone levels). Subjects signed a written informed consent. The study was approved by the local ethical committee.

Quantification of skin innervation

To quantify skin innervation originating from the three trigeminal branches (ophthalmic branch or V1, maxillary branch or V2 and mandibular branch or V3), 2-mm punch biopsies were taken immediately above the eyebrow and the upper lip and below the lower lip at the union of the outer with the middle third. A total of 48 samples were collected (18 from V1, 22 from V2 and 8 from V3). Fourteen subjects underwent biopsies from the first and the second branch, four from all three sites. The wound healed in a few days without a visible scar (Fig. 1).

Skin samples were processed using immunohistochemical techniques following previously described procedures (Kennedy & Wendelschafer-Crabb, 1993). Briefly, specimens were fixed overnight in Zamboni solution, cryoprotected in 20% sucrose in phosphate-buffered saline (PBS) and cut in 50-μm-thick sections using a freezing slide microtome (Leica 2000R, Wetzlar, Germany). Free floating sections were processed for indirect immunofluorescence using a panel of antibodies to mark neural and vascular structures (Table 1). Digital images were acquired using non-laser confocal microscopy (CARV confocal system; ATTO Biosciences, Rockville, MD, USA and Apotome confocal system; Zeiss, Oberkochen, Germany).

ENF density was evaluated according to international guidelines (Lauria et al., 2010a) applying NEUROLUCIDA software (MicroBrightField Bioscience, Williston, VT, USA) to four 20× z-series confocal images

Fig. 1 Wound healing in a 2-mm punch facial skin biopsy. The wound immediately after 2-mm punch skin biopsy in the perioral region. After 1 week the scar is hardly discernible.

(2 μm × 16 increments), obtained from four randomly selected sections for each sample. To quantify MFs, and to avoid sampling bias due to their uneven distribution in facial skin, since MFs cluster around hair follicles, we took into account the entire dermal surface included within 1 mm depth from the basement membrane in three random sections for each sample. The brightness and very low background of myelin basic protein (MBP) staining (Nolano et al. 2003; Provitera et al. 2007) ensured a very high signal/noise ratio and allowed MF counts on low magnification (5×) images of the entire section. We devised the following method: a calibrated grid (2 × 1 mm) with a series of seven equidistant parallel lines was applied on a digital non-confocal 5× image of MBP-stained sections. All intercepts between MF and the grid lines were counted (Fig. 2). When fiber overlapping made it difficult to identify the number of fibers, the designated area was double-checked using the epifluorescence microscope at a higher magnification.

The dermal area was calculated from the width of the section measured just below the epidermal-dermal junction and the grid depth (width × 1 mm depth), assuming that the conical shape of

Table 1 Abbreviation, source and dilution of immunohistochemical markers.

Antigen	Manufacturer and catalog number	Dilution
Protein gene product (PGP) 9.5	Biogenesis (Poole, UK) rabbit polyclonal #7863-0504	1 : 400
Vasoactive intestinal peptide (VIP)	Immunostar (Hudson WI, US) rabbit polyclonal # 20077	1 : 1000
Vasoactive intestinal peptide (VIP)	Santa Cruz Biotechnology (Heidelberg, Germany) mouse monoclonal # sc25347	1 : 300
Protein gene product (PGP) 9.5	AbD Serotec (Kidlington, UK) mouse monoclonal #7863-1004	1 : 800
Collagen IV (Col IV)	Chemicon (Billerica, MA, USA) mouse monoclonal #MAB1910	1 : 800
Substance P (Sub P)	Immunostar (Hudson WI, US) rabbit polyclonal #20064	1 : 1000
Calcitonin gene related peptide (CGRP)	Immunostar (Hudson WI, US) rabbit polyclonal #24112	1 : 1000
s100	Thermo Scientific Antibodies (Erembodegem, Belgium) rabbit polyclonal #RB-044-A0	1 : 10
Myelin basic protein (MBP)	Santa Cruz Biotechnology (Heidelberg, Germany) mouse monoclonal #sc-58542	1 : 800
Dopamine β hydroxilase (DβH)	Chemicon (Billerica, MA, USA) rabbit polyclonal #AB1536	1 : 150

our section was an artifact, due to dermis shrinkage. We accepted this method after comparing the results with those obtained by manually tracing the dermal area up to 1 mm in depth in 30 randomly selected sections using STEREOINVESTIGATOR software (MicroBrightField Bioscience) and finding excellent agreement with an intraclass correlation coefficient (ICC) = 0.97 ($P < 0.001$, lower 95% CI limit = 0.92). The limit of 1 mm of dermal depth for MF quantification was decided upon so as to exclude from the count, motor MF originating from the facial nerve and destined to striated muscle fibers, mostly located in the deeper dermis (Fig. 3).

MF density was calculated as the number of fibers intercepting the grid per area of dermis (intercepts per mm^2). A single operator blindly quantified all samples. Two weeks after the first measurements, the same operator and a second investigator blindly repeated the counts on 30% of samples to test intra- and interobserver reliability. In 30 randomly selected sections, we compared the results obtained by this method with those obtained using an unbiased stereological method as gold standard. Briefly, the total length of MF in the entire dermis volume included in 1 mm depth ($mm\ mm^{-3}$) was estimated using the 'space ball' (Fig. 2D–F) and 'Cavalieri estimator' probes of STEREOINVESTIGATOR software (Mouton et al. 2002; García-Fiñana et al. 2003). Twenty 20× confocal z-stack images were analyzed for each section.

Statistical analysis

All data are expressed as mean ± SD. Normal distribution of ENF and MF density values was evaluated using the Kolmogorov–Smirnov test. The *t*-test for paired and unpaired data was applied as appropriate. The linear correlation analysis was used to assess variable association as well as to compute the residual error around the regression line. The ICC with 95% confidence intervals (CI) between intra- and interobserver repeated measures was used to assess intra- and interobserver reliability. A P value ≤ 0.05 was considered statistically significant.

Results

Overall, the trigeminal skin appeared richly innervated (Fig. 4A). The epidermis was regularly populated by thin nerve fibers originating from a complex, vertically oriented, subepidermal plexus (Fig. 4B,C). The dermis contained a large number of annexes such as hair follicles (Fig. 4B), sebaceous and sweat glands (Fig. 4A). Hair follicles were heavily innervated by rich populations of unmyelinated and myelinated fibers (Fig. 4B–D). Approaching the hair follicle and after losing the myelin sheet, MFs repeatedly branched and terminated with expansions that assumed a tight palisade-like shape (Fig. 4E).

We frequently observed protein gene product (PGP)-ir fibers accompanying the hair follicle along its entire course, reaching the subepidermal plexus and entering the epidermis as free endings (Fig. 4C). In perioral samples, we occasionally observed other mechanoreceptors such as corpusculated Meissner-like receptors (Fig. 4F), Merkel complexes (Fig. 4G) and Ruffini-like receptors (Fig. 4H).

Vasoactive intestinal peptide (VIP)-ir fibers were abundant in the lower dermis around sweat glands, hair follicles, vessels and along the arrector pilorum muscle. Moreover, VIP-ir fibers were present in the upper dermis, around small arteries located in an unusual high position and reaching the papillary dermis. Finally, a peculiar and constant presence of VIP-ir fibers was found in the subepidermal plexus with some fibers approaching the epidermis (Fig. 5A–C). These fibers run close to the course of substance P (Sub-P) (Fig. 5B) and calcitonin gene related peptide (CGRP)-ir fibers (Fig. 5C) but without colocalization.

Fibers immunoreactive for dopamine β hydroxylase (DβH-ir) were present along arrector pilorum muscles and around vessels and sweat glands. However, compared with other parts of the body (Fig. 5F) DβH sudomotor fibers showed a denser pattern (Fig. 5E) and were more consistently present around sweat glands. CGRP and SubP-ir fibers appeared to be particularly abundant in the trigeminal territory, both in the dermis and in the epidermis. Furthermore, within the dermal layers of perioral samples, striated muscular fibers of the orbicularis oris muscle appeared scattered in the superficial dermis and organized in large bundles in the reticular

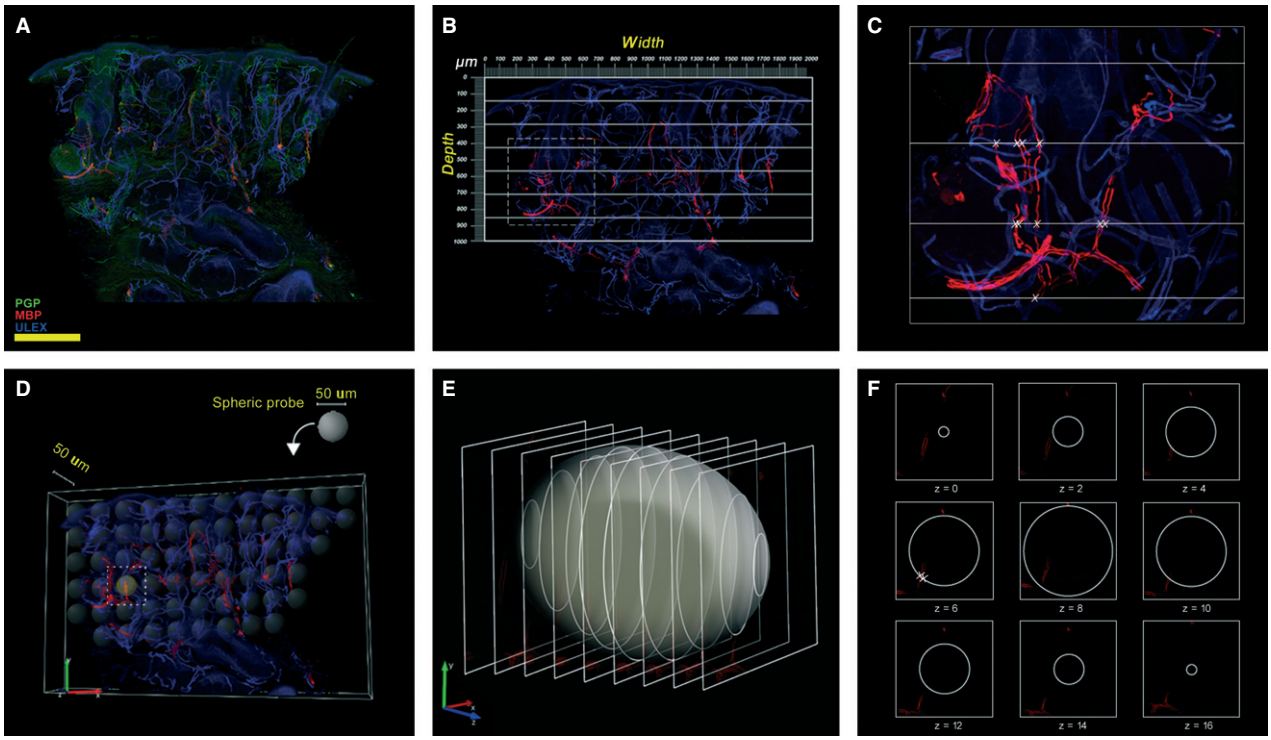

Fig. 2 Images exemplifying the methods used to quantify myelinated fibers. In green, PGP; in red, MBP; in blue, Ulex Europaeus agglutinin A. (A–C) Method used to quantify MF. (D–F), the unbiased stereological method used as gold standard in the field. (A) MBP/PGP/Ulex triple-stained 5× non-confocal image. Myelinated fibers are in red, axons are in green and epidermis and endothelium are in blue. (B) Application of a calibrated grid (2 × 1 mm) with a series of seven equidistant parallel lines on the same image using only the red and blue channels. (C) The area of tissue included in the square in (B) at higher magnification. The intersections between grid lines and fibers are marked with an X. Scale bar: 400 μm. (D) Distribution of virtual 'space ball' probes within the tissue. (E) Intersections between the probe and the confocal optical sections. (F) Intersections between nerve fibers and the probe are marked with an X.

dermis, about 1–1.5 mm under the basement membrane (Fig. 3A). Along muscular fibers it was possible to identify motor nerve fibers (Fig. 3B) and motor endplates (Fig. 3B,C).

Quantitative evaluation was performed on a total number of 336 sections (192 for ENF and 144 for MF). ENF density per mm was 23.0 ± 6.7 in V1, 20.7 ± 7.0 in V2 and 17.4 ± 4.5 inV3. MF density per mm^2 was 8.0 ± 3.6 in V1, 15.9 ± 6.5 in V2 and 16.4 ± 7.7 inV3 (Fig. 6A). Both ENF and MF densities in V1 differed ($P < 0.01$) from V2 and V3, whereas no difference was found between V2 and V3. Hence, we hereafter refer to the entire area innervated by V2 and V3 as perioral skin. ENF density decreased and MF density increased moving from the supraorbital to the perioral skin. Therefore, the two nerve fiber populations showed an opposite gradient and the ENF/MF ratio decreased from V1 (ENF/MF = 3.2 ± 1.3) to V2–V3 (ENF/MF = 1.5 ± 0.9).

ENF and MF density in both supraorbital and perioral skin correlated with age ($P < 0.01$ for ENF and $P < 0.05$ for MF). However, no gender-related difference in ENF or MF density was observed. A correlation ($P < 0.01$) between V1 and V2 ENF density was found in the 14 subjects who underwent skin biopsy from both sites (Fig. 6B).

Our method of MF quantification yielded an ICC of 0.97 for intraobserver reliability ($P < 0.001$, lower 95% CI limit = 0.93) and of 0.96 for interobserver reliability ($P < 0.001$, lower 95% CI limit = 0.92). A linear regression analysis between the results obtained with the 'grid' method and those obtained using the unbiased stereological approach yielded a high correlation coefficient ($r = 0.97$).

Discussion

To our knowledge this is the first morphological study of trigeminal cutaneous innervation in humans. It provides novel information about this complex territory and a quantitative assessment of ENF and dermal MF in the three divisions.

Sensory implications

In facial skin, we found a rich representation of sensory unmyelinated fibers in the epidermis (A delta and C endings) and MFs mainly directed to hair follicles, in the dermis (A beta fibers). This rich innervation may represent the

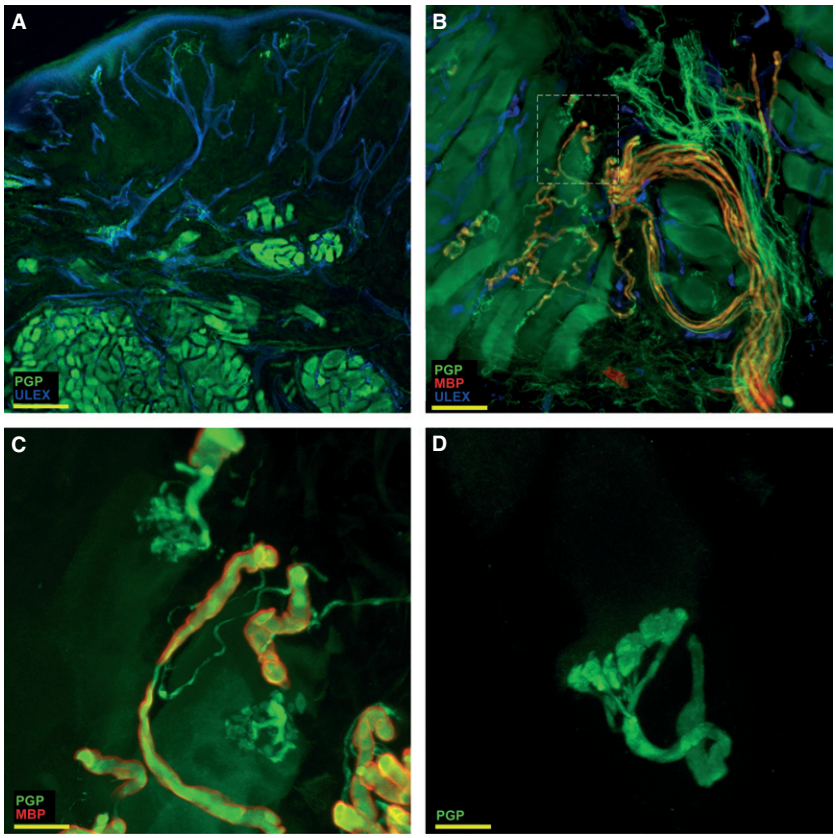

Fig. 3 Striated muscle in perioral skin. In the reticular dermis of perioral skin, about 1–1.5 mm below the basal membrane, evidence of striated muscular fibers from the orbicularis oris muscle (A) along with their motor nerve fiber endings and endplates (B). The detail marked with a square in B is shown at higher magnification in (C). (D) A motor endplate at 100× magnification. The images are taken from the second trigeminal branch. In green, PGP; in red, MBP; in blue, Ulex Europaeus agglutinin A. Scale bar: 400 μm (A), 65 μm (B), 50 μm (C), 20 μm (D).

morphological basis for the low threshold to thermal, noxious and tactile stimuli (Rolke et al., 2006), and for the easier recording of LEPs (Cruccu et al., 2003) in facial skin compared with the rest of the body. However, further morphological and immunohistochemical characterization of facial cutaneous fibers may be necessary to understand their functional peculiarities better.

The pattern of sensory innervation changes throughout the three divisions, and particularly between the supraorbital and perioral regions. In fact, moving from the supraorbital towards the more specialized perioral region, the density of ENF decreases predictably, as shown by the significant relationship between ENF density in V1 and V2 (Fig. 6B). Instead, moving from V1 to V2–V3, the density of MF increased with a reduction in ENF/MF ratio. This behavior resembles the pattern observed in the upper limbs where the lowest ENF/MF ratio occurs in the fingertip (Nolano et al. 2003). In this site the higher MF density occurs in parallel with the higher density of MC compared with proximal phalanx (Bolton et al. 1966; Caruso et al. 1994) and accounts for the higher tactile discrimination. Similarly, in facial skin, the higher perioral MF density (leading to a lower ENF/MF ratio) may contribute to the higher tactile detection, localization and discrimination ability of the perioral region compared with the more peripheral areas of the face (Cruccu et al. 2003; Hung & Samman, 2009).

This behavior may be related to the crucial role of the perioral region in the highly preserved activities implied in feeding and social interaction. In fact, although phylogenetically the role of the perioral region in environmental exploration has become less important with the evolution of the upper limb, this region remains pivotal for activities such as speech, chewing and swallowing. Accordingly, microneurographic studies in humans (Nordin et al. 1986; Trulsson & Johansson, 2002) have shown that mechanoreceptive afferents supplying the orofacial area (hair follicle fibers, fast-adapting receptors, and type I and type II slow-adapting receptors and afferent fibers) are strongly activated by mechanical stimulation due to contact between the lips, changes in air pressure during the speech and skin and mucosa deformations during chewing and swallowing activities.

Autonomic implications

The autonomic innervation in the trigeminal territory differs from other body sites due to its complexity and peculiarities. In particular, facial vasomotor control relies upon a mutual interaction of three sets of nerves: cranial parasympathetic, superior cervical sympathetic and trigeminal sensory nerves (Izumi, 1995, 1999). Among the several molecules involved in blood flow control (Charkoudian, 2010), VIP (Gibbins et al. 1984; Izumi, 1999) seems to play a main

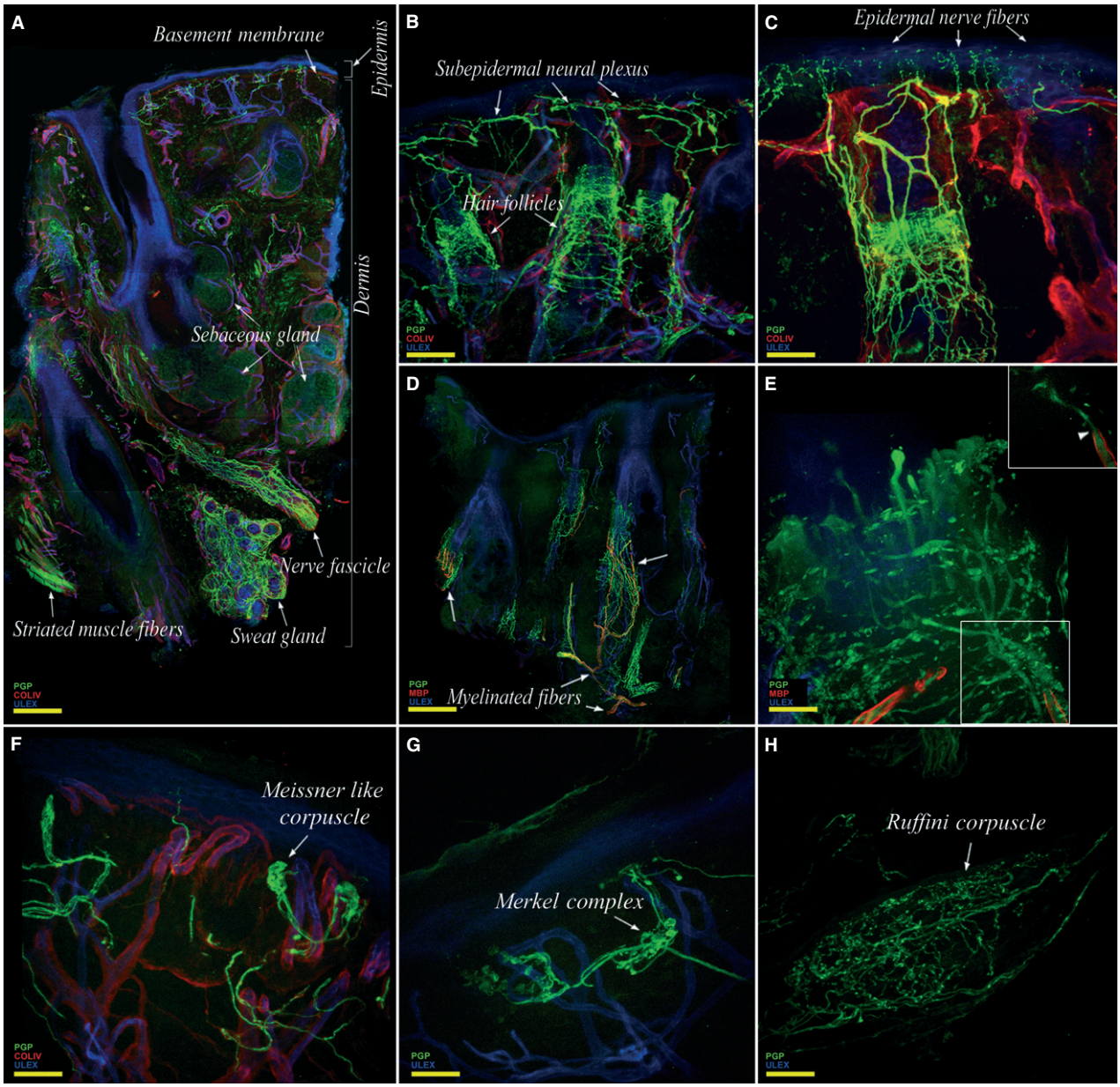

Fig. 4 Confocal images showing the complexity of cutaneous trigeminal innervation. (A) Collage showing an entire skin section with its rich dermal and epidermal innervation. (B) The abundance of hair follicles. (C) High density of epidermal nerve fibers. Hair follicles, the main mechanoreceptors of the hairy skin, are heavily innervated by unmyelinated fibers (C) and by myelinated fibers (D) that lose the myelinated sheet in proximity of their target, branch, and give origin to several neural expansions that envelop the hair follicle with a typical 'tight palisade' pattern (E). Mostly found in perioral skin, other mechanoreceptors such as Meissner-like corpuscles (F), Merkel complexes (G) and Ruffini receptors (H), are sometimes observed. The images are from the first (A) and the second trigeminal branch (B–H). In green, PGP; in red, collagen IV (A,B,C,F) and MBP (D,E); in blue, Ulex Europaeus agglutinin A. Scale bar: 220 μm (A,D), 200 μm (B), 100 μm (C,F), 50 μm (E,G,H).

role in facial skin. In addition to the usual presence of perivascular VIP-ir fibers in the lower dermis, we observed a constant and peculiar presence of VIP-ir fibers in the upper dermis. This superficial VIP-ir fiber contingent innervated very superficial small arterioles and capillary loops and participated in the sub-epidermal neural plexus, running along CGRP and SubP-ir fibers without colocalization. This distribution appears peculiar, because VIP in animal models has only been described in the upper dermis after experimental sensory nerve cuts (Ramien et al. 2004). Although, the exact role of these papillary VIP-ir fibers in the human face is unclear, they may be involved in in vasomotor control, particularly during blushing, mediating the emotional vasodilation (Goadsby & MacDonald, 1985; Drummond & Lance,

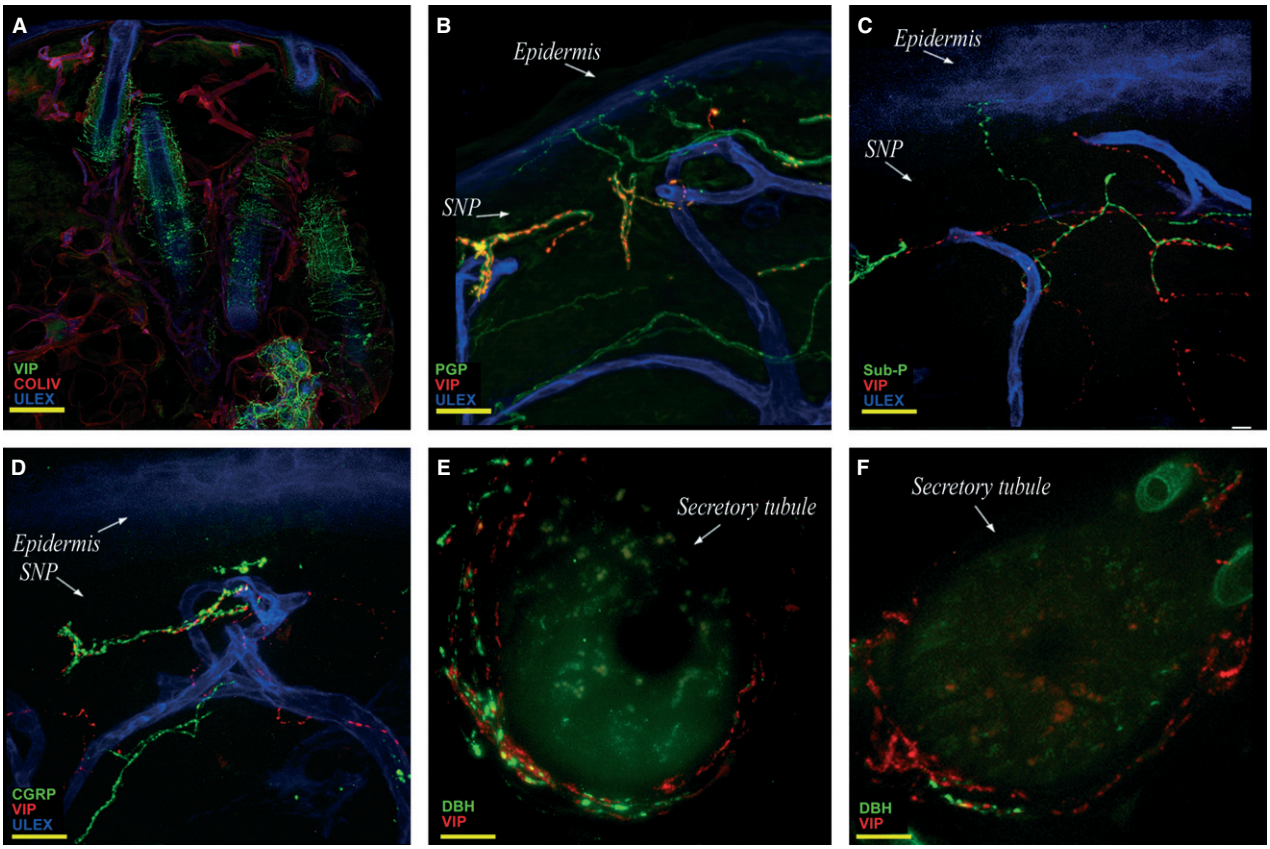

Fig. 5 Confocal images showing cutaneous autonomic innervation. (A) Collage showing VIP fiber distribution in the dermis around dermal annexes. (B,C,D) VIP-ir fibers in the SNP, in close contact with Sub P-ir fibers (C) and CGRP-ir fibers (D). Facial noradrenergic sudomotor innervation is consistently well represented (E) compared with non-facial body sites (F). Images are from the third (B–D) and the second trigeminal branch (A–E) and from the thigh (F). In green, VIP (A), PGP (B), Sub P (C), CGRP (D), DβH (E,F); in red, collagen IV (A), VIP (B–F); in blue, Ulex Europaeus agglutinin A. Scale bar: 160 μm (A), 100 μm (B); 50 μm (C,D); 20 μm (E,F).

1987). The strong expression of noradrenergic sudomotor nerves in facial skin, as shown by DβH immunoreactivity (DβH-ir), may represent the morphological basis of emotional sweating, as it is well known that in this territory, sweating goes beyond thermoregulatory function.

Methodology considerations

Using a 2-mm punch, we obtained a skin sample less than half the size of that obtained with the usually adopted 3-mm punch (3.14 vs. 7.07 mm^2 of skin surface). The 2-mm punch shows several advantages that make it particularly suitable for facial skin: a less noticeable wound, faster healing and a virtual absence of scarring. In spite of the small sample, to count ENF we considered the epidermal length of four instead of the standard three sections (Lauria et al. 2005).

Our approach to quantify MF proved to be satisfactory. Despite some promising attempts (Provitera et al. 2007; Doppler et al. 2012), quantification of MF in hairy skin is a difficult task because these fibers are scarce and unevenly distributed, as mentioned earlier. Such distribution leads to a wide variability among sections due to the inconstant presence of hair follicles. This anatomical condition would make it necessary to analyze several sections for each sample in order to obtain a reliable sampling of MFs. The task appeared relatively easier in facial skin, where the rich and constant presence of hair follicles ensured a good sampling of MF in our specimens. The distribution of these fibers, however, remained irregular within the same section. Therefore, to avoid sampling bias, we enlarged our region of interest to the whole dermis surface included in 1 mm depth from the basement membrane of three randomly selected sections. In fact, taking advantage of the brightness of the MBP-immunoreactivity we were able to use low magnification images.

This method, which requires a single nonconfocal 5× image, showed excellent agreement with the unbiased stereological method which requires the analysis of 20, 20× confocal images for each section. The agreement between the two series of measurements indicates that, regardless of the different spatial resolution, a reliable and accurate

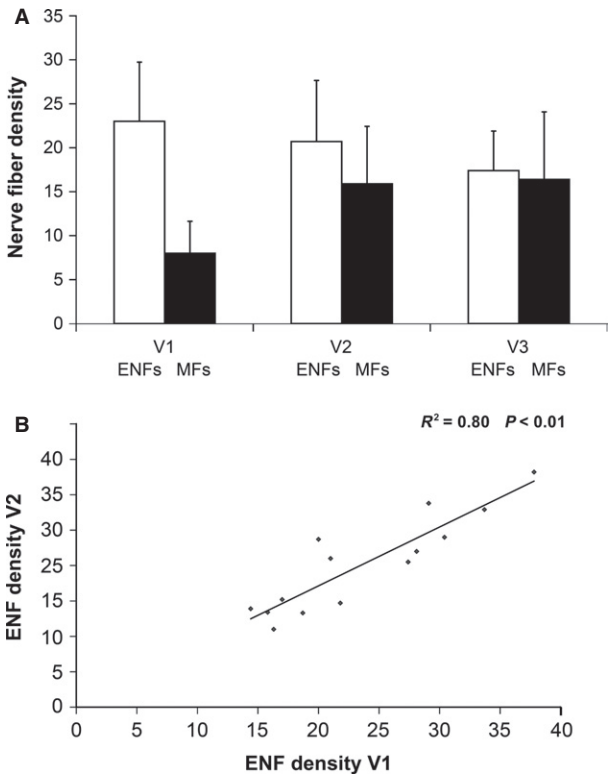

Fig. 6 Unmyelinated and myelinated fiber distribution in human facial skin. (A) Density of epidermal nerve fibers and myelinated fibers in the three trigeminal divisions. While epidermal nerve fiber density decreases from V1 to V2 and V3, myelinated fiber density increases showing an opposite gradient. ENF density is expressed in fibers mm^{-1}, MF density in intercepts mm^{-2}. (B) Relationship between epidermal nerve fiber density in V1 and V2. Data from the 14 patients who underwent skin biopsy from both V1 and V2 demonstrate a correlation between ENF density in the two sites.

quantification of MF in facial skin may be obtained from a single 5× image using the method we devised. Moreover, since this method doesn't require confocal microscopy, it is fast and it may be easily applied to brightfield immunohistochemistry.

Conclusions

Our morphological study on facial skin provides new insight into the normal trigeminal territory that has shown unique anatomical features. Facial skin is, in fact, hairy skin that shares some characteristics with glabrous skin (the abundance of annexes, the richness of innervation with plenty of mechanoreceptors and myelinated afferences). We also found neurochemical peculiarities of trigeminal cutaneous nerves that are unobserved in other skin areas or in homologous areas of lower species.

This can be related to the adaptive changes that have occurred in facial skin during the development of higher functions unique to the human species and mostly employed in communication, emotion and social interaction. In this light, we can also see the complexity of the cutaneous muscular supply. Indeed, the abundant presence of striated muscle and somatic motor nerve fibers is an additional peculiarity of facial skin. This anatomical characteristic is the basis of facial expression, and of non-verbal language that reaches its highest expression in humans and contributes to their communication abilities. The possibility of sampling striated muscle through perioral skin biopsy (Santoro et al., 2010) further broadens its clinical applications in pathologies involving muscle, motor nerve and motor endplate.

Finally, our study describes a tool with which to investigate the pathophysiological role of cutaneous afferences in different facial pain conditions, which are currently only studied by means of clinical and neurophysiological testing (Cruccu et al., 2003; Truini & Cruccu, 2008).

Author contributions

Study concept and design: Maria Nolano, Giorgio Cruccu, Lucio Santoro, Andrea Truini; acquisition of data: Maria Nolano, Vincenzo Provitera, Giuseppe Caporaso, Annamaria Stancanelli, Andrea Truini; analysis and interpretation of data: Maria Nolano, Vincenzo Provitera, Giorgio Cruccu, Lucio Santoro, Andrea Truini; drafting of the manuscript: Maria Nolano, Vincenzo Provitera, Andrea Truini; critical revision of the manuscript for important intellectual content: Maria Nolano, Vincenzo Provitera, Massimo Leandri, Antonella Biasiotta, Giorgio Cruccu, Lucio Santoro, Andrea Truini; statistical analysis: Maria Nolano, Vincenzo Provitera; administrative, technical and material support: Giuseppe Caporaso, Annamaria Stancanelli; study supervision: Maria Nolano.

References

Bolton CF, Winkelmann RK, Dyck PJ (1966) A quantitative study of Meissner's corpuscles in man. *Neurology* **16**, 1–9.

Caruso G, Nolano M, Lullo F, et al. (1994) Median nerve sensory responses evoked by tactile stimulation of the finger proximal and distal phalanx in normal subjects. *Muscle Nerve* **17**, 269–275.

Charkoudian N (2010) Mechanisms and modifiers of reflex induced cutaneous vasodilation and vasoconstriction in humans. *J Appl Physiol* **109**, 1221–1228.

Cruccu G, Pennisi E, Truini A, et al. (2003) Unmyelinated trigeminal pathways as assessed by laser stimuli in humans. *Brain* **126**, 2246–2256.

Cruccu G, Sommer C, Anand P, et al. (2010) EFNS guidelines on neuropathic pain assessment: revised 2009. *Eur J Neurol* **17**, 1010–1018.

Donadio V, Nolano M, Provitera V, et al. (2006) Skin sympathetic adrenergic innervation: an immunofluorescence confocal study. *Ann Neurol* **59**, 376–381.

Doppler K, Werner C, Henneges C, et al. (2012) Analysis of myelinated fibers in human skin biopsies of patients with neuropathies. *J Neurol* **259**, 1879–1887.

Drummond PD, Lance JW (1987) Facial flushing and sweating mediated by the sympathetic nervous system. *Brain* **110**, 793–803.

García-Fiñana M, Cruz-Orive LM, Mackay CE, et al. (2003) Comparison of MR imaging against physical sectioning to estimate the volume of human cerebral compartments. *Neuroimage* **18**, 505–516.

Gibbins IL, Brayden JE, Bevan JA (1984) Perivascular nerves with immunoreactivity to vasoactive intestinal polypeptide in cephalic arteries of the cat: distribution, possible origins and functional implications. *Neuroscience* **13**, 1327–1346.

Goadsby PJ, MacDonald GJ (1985) Extracranial vasodilation mediated by vasoactive intestinal polypeptide (VIP). *Brain Res* **329**, 285–288.

Howell K, Hopkins N, Mcloughlin P (2002) Combined confocal microscopy and stereology: a highly efficient and unbiased approach to quantitative structural measurement in tissues. *Exp Physiol* **87**, 747–756. Review.

Hung J, Samman N (2009) Facial skin sensibility in a young healthy Chinese population. *Oral Surg Oral Med Oral Pathol Oral Radiol Endod* **107**, 776–781.

Izumi H (1995) Reflex parasympathetic vasodilatation in facial skin. *Gen Pharmacol* **26**, 237–244. Review.

Izumi H (1999) Nervous control of blood flow in the orofacial region. *Pharmacol Ther* **81**, 141–161. Review.

Kennedy WR, Wendelschafer-Crabb G (1993) The innervation of human epidermis. *J Neurol Sci* **115**, 184–190.

Kennedy WR, Wendelschafer-Crabb G, Brelje TC (1994) Innervation and vasculature of human sweat glands: an immunohistochemistry-laser scanning confocal fluorescence microscopy study. *J Neurosci* **14**, 6825–6833.

Lauria G, Cornblath DR, Johansson O, et al. (2005) EFNS guidelines on the use of skin biopsy in the diagnosis of peripheral neuropathy. *Eur J Neurol* **12**, 747–758.

Lauria G, Hsieh ST, Johansson O, et al. (2010a) European Federation of Neurological Societies/Peripheral Nerve Society Guideline on the use of skin biopsy in the diagnosis of small fiber neuropathy. Report of a joint task force of the European Federation of Neurological Societies and the Peripheral Nerve Society. *Eur J Neurol***17**, 903–912, e44–49.

Lauria G, Bakkers M, Schmitz C, et al. (2010b) Intraepidermal nerve fiber density at the distal leg: a worldwide normative reference study. *J Peripher Nerv Syst* **15**, 202–207.

Mouton PR, Gokhale AM, Ward NL, et al. (2002) Stereological length estimation using spherical probes. *J Microsc* **206**, 54–64.

Nolano M, Provitera V, Crisci C, et al. (2003) Quantification of myelinated endings and mechanoreceptors in human digital skin. *Ann Neurol* **54**, 197–205.

Nordin M, Hagbarth KE, Thomander L, et al. (1986) Microelectrode recordings from the facial nerve in man. *Acta Physiol Scand* **128**, 379–387.

Provitera V, Nolano M, Pagano A, et al. (2007) Myelinated nerve endings in human skin. *Muscle Nerve* **35**, 767–775.

Ramien M, Ruocco I, Cuello AC, et al. (2004) Parasympathetic nerve fibers invade the upper dermis following sensory denervation of the rat lower lip skin. *J Comp Neurol* **469**, 83–95.

Rolke R, Baron R, Maier C, et al. (2006) Quantitative sensory testing in the German Research Network on Neuropathic Pain (DFNS): standardized protocol and reference values. *Pain* **123**, 231–243.

Santoro L, Nolano M, Faraso S, et al. (2010) Perioral skin biopsy to study skeletal muscle protein expression. *Muscle Nerve* **41**, 392–398.

Truini A, Cruccu G (2008) Laser evoked potentials in patients with trigeminal disease: the absence of A delta potentials does not unmask C-fibre potentials. *Clin Neurophysiol* **119**, 1905–1908.

Truini A, Galeotti F, Haanpaa M, et al. (2008) Pathophysiology of pain in postherpetic neuralgia: a clinical and neurophysiological study. *Pain* **140**, 405–410.

Trulsson M, Johansson RS (2002) Orofacial mechanoreceptors in humans: encoding characteristics and responses during natural orofacial behaviors. *Behav Brain Res* **135**, 27–33.